Research Square

Preprints are preliminary reports that have not undergone peer review.
They should not be considered conclusive, used to inform clinical practice,
or referenced by the media as validated information.

Ginsenoside Rg1 alleviates MAFLD by inhibiting oxidative stress and ferroptosis via the Nrf2/GPX4 pathway

Peiyun Peng
The First Affiliated Hospital of Chongqing Medical University
Kunli Yin
The First Affiliated Hospital of Chongqing Medical University
Zhijian Wang
The First Affiliated Hospital of Chongqing Medical University
Jia Zhang
The First Affiliated Hospital of Chongqing Medical University
Wenxiang Huang
wenxiang_huang@163.com
The First Affiliated Hospital of Chongqing Medical University

Research Article

Keywords: MAFLD, Rg1, Ferroptosis, Oxidative stress, Nrf2/GPX4

Posted Date: June 22nd, 2026

DOI: https://doi.org/10.21203/rs.3.rs-9770843/v1

License: This work is licensed under a Creative Commons Attribution 4.0 International License.
Read Full License

Additional Declarations: No competing interests reported.

Version of Record: A version of this preprint was published at European Journal of Medical Research on November 15th, 2026. See the published version at https://doi.org/10.1186/s40001-026-05497-0.

Abstract

Background

Metabolic dysfunction-associated fatty liver disease (MAFLD) imposes a significant global health burden, and safe and effective treatments are still lacking. Ginsenoside Rg1 (Rg1), a key bioactive compound extracted from ginseng, can effectively alleviate liver injury associated with MAFLD, but the specific molecular mechanism remains unclear.

Objective

This study aims to investigate the therapeutic effects of Rg1 on MAFLD and elucidate its underlying mechanisms.

Methods

A mouse model of MAFLD was established using the methionine-choline-deficient(MCD) diet, and Rg1 was given intragastrically for 4 consecutive weeks. The effects of Rg1 on MAFLD were investigated in vitro by cultivating HepG2 cells with free fatty acids (FFA). We used commercial assay kits, histopathological staining, transmission electron microscopy (TEM), immunofluorescence (IF), polymerase chain reaction (PCR), and Western blotting (WB) to assess parameters related to inflammation, oxidative stress, and ferroptosis in liver tissue and HepG2 cells. Molecular docking and the Nrf2 inhibitor (ML385) were used to validate the potential mechanisms underlying the hepatoprotective effects of Rg1.

Results

Rg1 treatment dramatically reduced hepatic Fe^{2+}, oxidative stress, and inflammatory factor levels. In vitro experiments revealed that Rg1 reduced iron, MDA, and ROS levels, while upregulating SLC7A11 and GPX4 to inhibit oxidative stress and ferroptosis. These results suggest that Rg1 exerts antioxidant and anti-ferroptotic effects by activating the Nrf2/GPX4 signaling pathway.

Conclusion

Rg1 is a natural bioactive compound with potential therapeutic applications for MAFLD; it inhibits hepatic ferroptosis, reduces oxidative stress, and alleviates MAFLD by activating the Nrf2/GPX4 pathway.

1. Introduction

Metabolic dysfunction-associated fatty liver disease (MAFLD) has become the most common cause of chronic liver disease, posing a severe threat to human health [1]. Due to the prevalence of obesity and diabetes, the prevalence of MAFLD has been increasing year by year. Currently, the global prevalence of MAFLD in adults is approximately 32%, affecting nearly 2 billion people worldwide [2]. MAFLD encompasses a range of liver diseases, from simple steatosis to metabolic dysfunction-associated steatohepatitis(MASH), which can progress to liver fibrosis, cirrhosis, and even hepatocellular carcinoma (HCC). The pathogenesis of MAFLD is not fully elucidated. The widely accepted ”multiple-hit” theory suggests that its progression involves interactions among genetic factors, environmental factors, metabolic disorders, inflammation, and the gut microbiota [3]. Due to the complex pathological mechanism of MAFLD, there is still a lack of effective treatments.

Ferroptosis, a novel form of programmed cell death, is characterized by intracellular iron overload, excessive accumulation of reactive oxygen species(ROS), and lipid peroxidation [4]. When there is an excess of iron in the liver, excess free iron can generate hydroxyl radicals and ROS through the Fenton reaction [5]. ROS damages liver cells and exacerbates inflammation and oxidative stress. Iron-induced lipid peroxidation promoting hepatocyte ferroptosis is considered an important factor in the progression of MAFLD [6]. Patients with MAFLD exhibit elevated levels of lipid peroxidation markers MDA and 4-HNE, along with decreased Nrf2 levels [7]. In a mouse model, the GPX4 activator selenite and the ferroptosis inhibitor Liproxstatin-1(Lip-1) suppressed ferroptosis, attenuated the inflammatory response, and alleviated MASH; conversely, the ferroptosis inducer RSL3 downregulated GPX4 levels and exacerbated MASH [8]. In summary, these studies suggest that inhibiting ferroptosis may be a promising strategy for treating MAFLD.

The nuclear factor erythrocyte 2-associated factor 2(Nrf2) is a key regulator of antioxidant responses, maintaining cellular redox homeostasis by activating antioxidant response elements(ARE) in stress-response genes [9]. GPX4 is a phospholipid peroxidase and a direct downstream target of the Nrf2 antioxidant pathway [10]. It mitigates oxidative damage by reducing lipid hydroperoxides(L-OOH) to corresponding alcohols(L-OH) to maintain cell membrane stability and inhibit ferroptosis [11, 12]. Previous studies demonstrated that the Nrf2/GPX4 is a key signaling pathway inhibiting ferroptosis, and recent research shows Nrf2 alleviates MASH via upregulating GPX4 [13].

Ginseng is a traditional Chinese herbal medicine with a variety of pharmacological effects, including anti-inflammatory and antioxidant properties, as well as benefits for promoting liver function recovery [14]. Rg1 is a single compound extracted from ginseng and plays a positive role in the treatment of various liver diseases [15, 16]. Related studies have reported that Rg1 activates the Nrf2 signaling pathway, thereby alleviating LPS-induced chronic liver injury [17)]. In addition, Rg1 can also improve CCl_4-induced liver fibrosis [18]. These studies highlight the potential of Rg1 in the treatment of liver diseases via ferroptosis inhibition, but its specific mechanism in the treatment of MAFLD, particularly its relationship with ferroptosis, remains unclear, which may be related to the Nrf2 signaling axis.

In this study, we evaluated the therapeutic effects of Rg1 on MAFLD and clarified its role in regulating ferroptosis via the Nrf2/GPX4 axis. This provides new mechanistic insights and experimental evidence for the treatment of MAFLD.

2. Materials and methods

2.1 Animals and experimental design

Male C57BL/6J mice (6 weeks old) were purchased from Ensweier Biotechnology Co., Ltd. (Chongqing, China). The temperature in the control room was maintained between 21 and 23℃, and the humidity between 50 and 60%. During this period, the mice were fed a standard diet and provided with ad libitum sterile water. After a 7-day acclimatization period, the animals were randomly divided into four groups (n = 6): Control group: Dietary group receiving methionine and choline supplements (MCS). Model group: MCD diet group. MCD+Rg1 low-dose group (L). MCD+Rg1 high-dose group (H). Mice were fed an MCD diet for 6 consecutive weeks to establish a mouse model of MAFLD. Based on the results of previous studies and literature review, mice received continuous gavage of Rg1(60 and 120mg/kg.d) for 4 weeks after a 2-week MCD diet [15, 19, 20]. Mice were anesthetized by intraperitoneal injection of sodium pentobarbital at a dosage of 50 mg/kg. The eyeballs of mice were removed for blood collection. Next, mice under deep anaesthesia were humanely euthanized via an overdose of sodium pentobarbital to collect liver specimens in accordance with animal welfare guidelines. All animal protocols for this study have been approved by the Animal Ethics Committee of Chongqing Medical University(Approval No. IACUC-CQMU-2025-07039).

2.2 Biochemical assays

ALT, AST, TC, TG, iron, SOD, and GSH levels were measured using commercially available assay kits according to the instructions(Jiancheng Co., Ltd., Nanjing, China). Quantification of inflammatory mediators(TNF-α, IL-6, and IL-1β), MDA, and Fe^{2+} was performed by enzyme-linked immunosorbent assay (ELISA) using the assay kit(Elabscience Biotechnology Co., Ltd, Wuhan, China).

2.3 Histopathological analysis

Liver tissue was fixed in 4% paraformaldehyde for 48 hours, dehydrated, and embedded in paraffin. Then slice the tissue into 4 μm sections. Deparaffinization, rehydration, and staining of tissue sections using the HE kit, Masson´s kit(Solarbio, Beijing, China), and Sirius Red kit(Leagene Biotech, Beijing, China). To measure total iron in the liver, liver slices were stained using a Prussian blue iron staining kit(Solarbio, Beijing, China). The samples were incubated with Perls staining buffer for at least 30 minutes, and histological images were captured using an Olympus optical microscope.

2.4 Cell culture and treatment

HepG2 cells(Servicebio, Wuhan, China)were cultured in high-glucose DMEM containing 10% fetal bovine serum, 100 U/mL penicillin, and 100 μg/mL streptomycin in a 37°C, 5% CO_2 incubator. Mixed oleic acid

and palmitic acid in a 2:1 ratio, then dissolved the mixture in a medium containing 1% bovine serum albumin (BSA) to produce a 1 mM free fatty acids(FFA) solution. To establish a MASH cell model, HepG2 cells were treated with 1 mM FFA for 24 hours. When cell density reached 50%, the cells were treated simultaneously with different concentrations of Rg1 (25 and 50 μM) and erastin (10 μM) for 24 hours to evaluate the effects of Rg1 and ferroptosis on MAFLD. Additionally, HepG2 cells were co-incubated with ML385 (MCE, USA) to inhibit Nrf2 expression.

2.5 Cell counting kit-8 (CCK8) determination

Rg1 was added to HepG2 cells after being dissolved in DMSO. 5×103cells were seeded in a 96-well plate and then incubated with different concentrations of Rg1 or FFA. Cell viability was assessed using the CCK-8 assay(Beyotime, Shanghai, China).

2.6 Oil red O staining for lipid accumulation

Frozen liver samples were embedded in OCT compounds and cut into 10μm sections, or cultured cells were seeded onto slides. The slices were rinsed with distilled water, stained with Oil Red O working solution for 30 minutes, and then differentiated in 60% isopropanol to remove excess Oil Red O solution. Cell nuclei were counterstained with hematoxylin. Finally, the samples were covered with a coverslip and observed under an optical microscope (Olympus IX73, Tokyo, Japan).

2.7 Measurement of ROS production

Cellular ROS levels were measured using the fluorescent probe DCFH-DA(Beyotime, Shanghai, China). Add 10 μM DCFH-DA to the treated cells and incubate in the dark at 37°C for 30 minutes. After washing, fluorescence images were obtained using a confocal microscope(Nikon Corporation, Tokyo, Japan).

2.8 Immunofluorescence staining

After dewaxing, hydration, antigen retrieval, and BSA blocking, the paraffin sections were incubated overnight at 4°C with α-SMA(1: 200; Selleck, USA, Cat #L19D14) and collagen I (1: 400; Proteintech, China, Cat #67288-1)antibodies, respectively. The following day, they were incubated with the corresponding fluorescent secondary antibody (Alexa Fluor 594) at room temperature under dark conditions for two hours, and then stained with DAPI for five minutes. Finally, the slides were mounted with an anti-fluorescent quencher, and the corresponding fluorescence was observed.

HepG2 cells were seeded in confocal laser culture dishes, rinsed with phosphate-buffered saline (PBS), fixed with 4% paraformaldehyde for 20 minutes, and then permeabilized with 0.5% Triton X-100 and 5% BSA. After permeabilization, the cells were incubated overnight with GPX4 antibody(1: 200; Proteintech, China, Cat #30388-1), Nrf2 antibody(1: 400; Proteintech, China, Cat #80593-1), and HO-1 antibody(1: 200; Proteintech, China, Cat #66743-1) at 4 ℃, with Nrf2 and HO-1 being co-stained. The next day, the corresponding secondary antibodies (GPX4: Alexa Fluor 488; Nrf2: Alexa Fluor 594; HO-1: Alexa Fluor 488) and DAPI were incubated. Images were acquired using a Nikon confocal microscope.

2.9 Western blot (WB)

Total protein was extracted using RIPA(Beyotime, China), phosphatase inhibitors, and PMSF(Beyotime, China). Protein concentration was quantified using a BCA protein assay kit(Beyotime, China), followed by denaturation. The samples were subjected to SDS-PAGE gel and transferred to PVDF membrane(Millipore, USA). The membrane was blocked with 5% skim milk, then incubated with the primary antibody overnight at 4℃. The primary antibodies used were as follows:collagen I(1: 5000; Proteintech, China, Cat #67288-1),α-SMA(1: 1000; Selleck, USA, Cat #L19D14),GAPDH(1: 5000; Proteintech, China, Cat #10494-1),GPX4(1: 500; Proteintech, China, Cat #30388-1),SLC7A11(1: 5000; Proteintech, China, Cat #82115-3),TNF-α(1: 1000;CST, USA, Cat #3707),IL-6(1: 500; Proteintech, China, Cat #21865-1),Nrf2(1: 1000; Proteintech, China, Cat #80593-1),and HO-1(1: 1000; Proteintech, China, Cat #66743-1). After TBST washing, it was reacted with HRP-labeled secondary antibody at room temperature for 1 hour, and then the membrane was detected. Protein samples were visualized using the ECL kit (Beyotime, China) and analyzed using ImageJ software.

2.10 Observation of mitochondria via transmission electron microscopy (TEM)

Fresh liver tissue or HepG2 cells were fixed in 2.5% glutaraldehyde(4℃,2h), the fixative was discarded, the cells were soaked in PBS buffer for 2 hours, and then 1% osmium tetroxide was added for fixation for 1 hour. They were dehydrated using a series of ethanol gradients, embedded in epoxy resin, and sectioned on a microtome (70 nm). Stained sections were imaged at high magnification to observe the integrity of mitochondrial cristae and cell membranes.

2.11 Molecular docking

The binding mode of Rg1 and Nrf2 was investigated using molecular docking. The crystal structure of Nrf2 was retrieved from the RCSB Protein Data Bank(https://www.rcsb.org/). The structure of Rg1 was obtained from the PubChem database(https://pubchem.ncbi.nlm.nih.gov/).

Molecular docking was performed using AutoDock Vina 1.5.6, and the conformation with the highest number of repetitions and the best binding affinity was selected as the output result.

2.12 Quantitative real-time polymerase chain reaction (qRT- PCR)

Total RNA was extracted from HepG2 cells using TRIzol reagent(Invitrogen, USA). RNA concentration was measured using Nanodrop 2000C(Thermo Scientific, USA). Subsequently, we used the ReverTra Ace qPCR RT Kit(Takara, Tokyo, Japan)to reverse-transcribe the RNA into cDNA.

qPCR was performed using the SYBR® Green Premix Pro-Taq HS qPCR Kit (Accurate Biotechnology, China) on the CFX96 system (Bio-Rad, USA). The primers(Sangon Biotech, China) for HepG2 cells are listed in Table 1. Relative mRNA expression levels were calculated using the $^{2-\triangle\triangle}$Ct method. All target genes were standardized with β-actin.

Table 1
Primer Sequences for qRT-PCR.

Primer	Forward	Reverse
β-actin	CCCATCTATGAGGGTTACGC	TTTAATGTCACGCACGTTC
Nrf2	TCTTCTGTGCTGTCAAGGG	CTCTTTCCGTCGCTGACT
HO-1	GTGACCCGAGACGGCTT	ACAGGGGCGAAGACTGG
GPX4	TTGCCGCCTACTGAAGC	ATGTGCCCGTCGATGTC

2.13 Statistical analysis

Statistical analyses were performed using GraphPad Prism 10.0 software. All data were repeated at least 3 times and expressed as the mean±standard deviation(SD). One-way analysis of variance (ANOVA) was used to analyze the differences between groups, and $p < 0.05$ was considered statistically significant.

3. Results

3.1 Rg1 improves liver function and reduces liver injury in the MCD model mice.

Mice were fed an MCD diet to establish an MAFLD model for 6 weeks and then received Rg1 (60 mg/kg or 120 mg/kg) via oral gavage for 4 weeks. The animal experimental protocol is illustrated in Fig. 1A. The MCD diet resulted in a significant body weight and liver weight loss in mice. Rg1 treatment failed to alleviate MCD-induced weight and liver reduction(Fig. 1B). Rg1 can dramatically decrease the levels of serum ALT and AST, as well as liver TC and TG, compared with the model group(Fig. 1C-D). As shown in Fig. 1E, the model group exhibited hepatocyte ballooning, inflammatory cell infiltration, lipid deposition, fibrotic scarring, and collagen deposition, while these phenomena were significantly reduced after Rg1 treatment. Additionally, Rg1 also reduced the fluorescence intensity of α-SMA(Fig. 1F).

3.2 Rg1 enhances antioxidant capacity, reduces inflammation, and alleviates ferroptosis.

The levels of serum MDA and serum inflammatory factors (IL-6, IL-1 β, TNF - α) in the model group were significantly higher compared to controls, whereas the levels of serum SOD and GSH were considerably lower. Rg1 dose-dependently reduced levels of inflammatory cytokines and MDA in mice, while increasing levels of the antioxidants SOD and GSH(Fig. 2A,2C-E). Furthermore, Rg1 treatment reduced the elevated Fe^{2+} content in hepatocytes caused by the MCD diet(Fig. 2B). Hepatic iron deposition decreased after Rg1 medication, according to Prussian blue staining(Fig. 2F). Transmission electron microscopy (TEM) results showed that mice in the MCD group exhibited a substantial decrease in mitochondrial cristae and an increase in mitochondrial membrane density; these findings improved after

Rg1 treatment(Fig. 2G). Our Western blot results suggested that the expression of SLC7A11 and GPX4, the pivotal proteins involved in the redox pathway of ferroptosis, is also upregulated by Rg1(Fig. 2H-I).

3.3 Rg1 inhibits FFA-induced ferroptosis in HepG2 cells.

The results in Fig. 3A demonstrated that Rg1 has virtually no toxic effect on HepG2 cells. When the Rg1 concentration was 75μM, there was a difference in the number of surviving HepG2 cells. (Fig. 3A). Therefore, concentrations of 25 μM and 50 μM were selected for subsequent testing to avoid the cytotoxic effects of Rg1. Similarly, the toxicity of FFA to HepG2 cells was assessed using the CCK-8 assay. The results showed that FFA toxicity to HepG2 cells was concentration-dependent; as the FFA concentration increased, cell viability gradually decreased (Fig. 3B). 1mM FFA was determined to establish a lipotoxic environment in subsequent experiments. In Rg1-treated HepG2 cells, iron levels and lipid peroxidation products were observed to be reduced, while the antioxidant capacity was enhanced(Fig. 3C-3F). TEM analysis revealed that the mitochondrial volume of HepG2 cells treated with Rg1 gradually returned to normal, and the number of mitochondrial cristae increased, indicating an improvement in ferroptosis (Fig. 3G). Moreover, immunofluorescence staining suggested that GPX4 expression showed significant up-regulation following treatment with Rg1(Fig. 3H).

3.4 Induction of ferroptosis exacerbates FFA-induced lipid accumulation in HepG2 cells.

To further investigate the role of Rg1 in alleviating ferroptosis in MASH, the ferroptosis inducer Erastin was used to induce ferroptosis in HepG2 cells. We found that Rg1 treatment increased GSH levels and reduced iron, MDA, and ROS levels in HepG2 cells, whereas erastin increased the levels of these ferroptosis markers(Fig. 4A-D). WB results showed that Rg1 treatment increased the expression of GPX4 and SLC7A11 and decreased the expression of TNF-α and IL-6 in HepG2 cells; this phenomenon was reversed by Erastin(Fig. 4E-F). In addition, the results of TC and TG measurements and Oil Red O staining also suggested that promoting ferroptosis can exacerbate FFA-induced lipid deposition in HepG2 cells (Fig. 4G-H).

3.5 Rg1 activates the Nrf2/GPX4 signaling pathway in HepG2 cells

The molecular docking results showed that Rg1 exhibited a high binding affinity with Nrf2 protein, with a predicted binding energy of -6.7 kcal/mol, indicating a strong interaction between the ligand and the protein (Fig. 5A). Rg1 significantly increased the mRNA and protein expression of Nrf2, HO-1, and GPX4 in FFA-induced HepG2 cells, and this effect was dose-dependent(Fig. 5B-D, F-G). The expression levels of Nrf2, HO-1, and GPX4 at both the protein and mRNA levels indicated that the inhibition of ferroptosis by Rg1 is closely associated with the Nrf2/GPX4 signaling pathway. Furthermore, immunofluorescence staining revealed that the protein expression of Nrf2 and GPX4 was highly consistent, and their expression was enhanced by Rg1 treatment, implying the translocation of Nrf2 to the cell nucleus and activating the Nrf2/GPX4 pathway, thereby inhibiting ferroptosis(Fig. 5E).

3.6 The Nrf2/GPX4 pathway is a key pathway for Rg1 to inhibit lipid deposition and oxidative stress in HepG2 cells.

To clarify whether the Nrf2/GPX4 signaling pathway is a key pathway for Rg1 to improve MAFLD, we used the Nrf2 inhibitor (ML385) to inhibit Nrf2 transcription in HepG2 cells. Assessments of iron, MDA, SOD, and GSH levels in HepG2 cells showed that iron and MDA levels in the Rg1-treated group considerably increased after ML385 administration, whereas SOD and GSH levels dramatically reduced (Fig. 6A-6D). Oil Red O staining and ROS detection data were consistent with these results(Fig. 6E-6F). This study also suggested that the expression of Nrf2 and GPX4 proteins in HepG2 cells was significantly reduced when ML385 was added(Fig. 6G-6H). Therefore, we speculate that Rg1 may target the Nrf2/GPX4 signaling pathway to inhibit FFA-induced oxidative stress and ferroptosis in HepG2 cells, thereby reducing lipid accumulation(Fig. 7).

4. Discussion

MAFLD is a potentially serious condition that poses a significant threat to public health, whose prevalence is on the rise. In 1998, Day and James were the first to propose the classic “two-hit” theory to explain the pathogenesis of MAFLD [21]. This hypothesis suggests that the first mechanism involves lipid accumulation in the liver and insulin resistance, while the second mechanism is oxidative stress. However, subsequent research has shown that the traditional “two-hit” theory is no longer sufficient to explain the complex pathogenesis of MAFLD. Therefore, the "multiple-hit" theory has been proposed. Based on this theory, insulin resistance, lipotoxicity, endoplasmic reticulum stress, inflammation, mitochondrial dysfunction, oxidative stress, gut microbiota, and genetic factors all contributed to MAFLD [3, 6, 22]. Despite numerous clinical and basic research studies conducted in recent years, the detailed molecular mechanisms underlying the pathogenesis of MAFLD remain to be elucidated, and there is a lack of approved therapeutic strategies. Related studies have shown that ferroptosis is associated with the onset of early-stage steatohepatitis in MASH mouse models; inhibiting ferroptosis can significantly alleviate MASH [23]. Traditional Chinese medicine (TCM) exerts a holistic regulatory effect through multiple targets, and its advantages in the treatment of MAFLD are becoming increasingly evident. In this study, we clarified the effects of Rg1 on MAFLD both in vivo and in vitro. The result showed that Rg1 suppresses ferroptosis and alleviates liver injury by activating the Nrf2/GPX4 pathway.

Rg1, a well-known tetracyclic triterpenoid of the 20(S)-protopanaxatriol type [24], is abundant and bioactive in ginseng, which plays a major role in its pharmacological effects. Rg1 has been shown to have good therapeutic effects in the treatment of a variety of disorders. These effects include anti-inflammatory and antioxidant qualities as well as the capacity to regulate ferroptosis. In the diabetic cardiomyopathy model, Rg1 suppressed inflammation response, decreased NF-κB and NLRP3 inflammasome expression, and increased PGC-1α, complex III, and complex □ expression to promote mitochondrial biogenesis, thereby alleviating cardiac hypertrophy and hypertension [25]. Notably, Rg1 treatment attenuated D-gal-induced testicular injury in vivo and in vitro models by enhancing Akt phosphorylation and reducing oxidative stress [26]. Our previous studies have shown that Rg1 has a

protective effect against both alcoholic liver disease (ALD) and CC14-induced liver fibrosis [15, 18]. The present study indicates that Rg1 reduces oxidative stress indicators and inflammatory cytokines while also suppressing ferroptosis, suggesting that ferroptosis inhibition may be a promising therapeutic approach for MAFLD.

Oxidative stress leads to cellular dysfunction, causing simple hepatic steatosis to progress to steatohepatitis, which is considered an important factor in the progression of MAFLD [27, 28]. Ferroptosis plays a key role in regulating lipid metabolism and is the primary cell death mechanism in the pathogenesis of MAFLD [29]. When iron overload occurs, excessive ferrous ions in cells can cause lipid peroxidation through the Fenton reaction, leading to oxidative stress, metabolic disorders, and promoting the occurrence of MAFLD [30, 31]. Recent studies have shown that targeting ferroptosis can significantly slow the progression of MAFLD, including reducing hepatic steatosis, inflammation, and fibrosis [32]. As a non-hepatotoxic traditional Chinese medicine monomer, Rg1 exhibits anti-inflammatory effects on FFA-induced HepG2 cells and reduces the production of iron, ROS, and MDA, suggesting that Rg1 can inhibit FFA-induced oxidative stress and ferroptosis. Kong et al. demonstrated that Rg1 has antioxidant properties and protects neurons from ferroptosis in chronic inflammatory neurodegenerative diseases (NDDs), which is consistent with our findings [33]. However, it is not fully clear whether and how Rg1 alleviates ferroptosis in MAFLD.

Nrf2 is the main transcription factor regulating oxidative stress response, involved in various biological processes such as antioxidant response, iron metabolism, the maintenance of normal mitochondrial function, and apoptosis [34]. Under basal conditions, Keap1 in the cytoplasm binds to Nrf2 and mediates its degradation through the ubiquitin-proteasome pathway, thereby inhibiting its activity. During oxidative stress, Nrf2 is released from Keap1 and translocates to the nucleus, where it binds to antioxidant response elements(ARE) and initiates the transcription of downstream antioxidant genes (HO-1 and GPX4) [35, 36]. Studies have confirmed that Rg1 exerts anti-inflammatory and antioxidant effects by activating Nrf2 [37, 38]. Activation of the Nrf2 pathway shows great promise in the treatment of MAFLD. Esculin and Gaudichaudione H improved liver fibrosis and inflammation by enhancing Nrf2 signaling [39, 40]. Animal studies suggested that liver injury associated with MAFLD was exacerbated in Nrf2-knockout mice, highlighting the critical role of Nrf2 in the pathogenesis of MAFLD [41]. This study further verified the relationship between Nrf2 and MAFLD, as well as the strong affinity between Rg1 and Nrf2, using molecular docking.

GPX4 is an antioxidant enzyme that converts toxic lipid peroxides into non-toxic lipidiols, thereby inhibiting lipid peroxidation and playing a crucial role in the process of ferroptosis [42]. The Nrf2/GPX4 signaling pathway is a key signaling pathway that mediates ferroptosis [43]. Based on the relationship between Rg1 and Nrf2, we hypothesize that the beneficial effects of Rg1 on MAFLD are mediated by activating the Nrf2/GPX4 signaling pathway. The results showed that levels of Nrf2 and GPX4 were significantly reduced in HepG2 cells in the model group, and expression of HO-1, a downstream protein in the Nrf2 signaling pathway, was also decreased. Following treatment with Rg1, Nrf2/GPX4 signaling

pathway-related factors were upregulated. Furthermore, the inhibitory effects of Rg1 on oxidative stress and ferrocytosis in HepG2 cells were reversed by the Nrf2 inhibitor ML385.

Our study confirms that Rg1 has certain potential in the treatment of MAFLD, but its limitations still need to be considered. Future studies could conduct genetic validation (knockdown/overexpression) and incorporate multi-omics analysis to provide further robust mechanistic evidence, demonstrating that Rg1 alleviates MAFLD by specifically interfering with the Nrf2/GPX4 axis.

In conclusion, this study suggests that Rg1 improves MAFLD by inhibiting ferroptosis, oxidative stress, and alleviating inflammation and lipid accumulation by regulating the Nrf2/GPX4 axis. This finding provides a new approach and theoretical basis for MAFLD treatment.

Abbreviations

MAFLD	Metabolic dysfunction-associated fatty liver disease
Rg1	Ginsenoside Rg1
MCD	Methionine-choline-deficient
FFA	Free fatty acids
TEM	Transmission electron microscopy
IF	Immunofluorescence
PCR	Polymerase chain reaction
WB	Western blotting
MASH	Metabolic dysfunction-associated steatohepatitis
HCC	Hepatocellular carcinoma
ROS	Reactive oxygen species
Nrf2	The nuclear factor erythrocyte 2-associated factor 2
ARE	Antioxidant response elements
TCM	Traditional Chinese medicine
NDDs	Neurodegenerative diseases
ALD	Alcoholic liver disease

Declarations

Clinical trial number: not applicable.

Author Contributions

Conception and design of the research: Wenxiang Huang; Acquisition and analysis of data: Zhijian Wang and Jia Zhang; The drafting and writing of the manuscript: Peiyun Peng. The revision of the manuscript: Kunli Yin. All authors read and approved the final manuscript.

Funding

This work was supported by the Chongqing Medical Key Discipline and Regional Medical Key Discipline Development Project (0201 [2024] No. 136202550).

Availability of data and material

The data that support the findings of this study are available from the corresponding author upon reasonable request.

Ethics approval

All experimental procedures were approved by the Institutional Animal Care and Use Committee of Chongqing Medical University. All animal housing and experiments were conducted in strict accordance with the institutional guidelines for care and use of laboratory animals.

Consent for publication

No individual patient data are presented in this paper, and consent for publication was not required.

Competing interests

The authors declare no competing interests.

References

1. Teng ML, Ng CH, Huang DQ, Chan KE, Tan DJ, Lim WH, et al. Global incidence and prevalence of nonalcoholic fatty liver disease. Clin Mol Hepatol. 2023;29(Suppl):S32–s42.
2. Riazi K, Azhari H, Charette JH, Underwood FE, King JA, Afshar EE, et al. The prevalence and incidence of NAFLD worldwide: a systematic review and meta-analysis. Lancet Gastroenterol Hepatol. 2022;7(9):851–61.
3. Loomba R, Friedman SL, Shulman GI. Mechanisms and disease consequences of nonalcoholic fatty liver disease. Cell. 2021;184(10):2537–64.
4. Zhou Z, Li J, Zhang X. Natural Flavonoids and Ferroptosis: Potential Therapeutic Opportunities for Human Diseases. J Agric Food Chem. 2023.
5. Conrad M, Pratt DA. The chemical basis of ferroptosis. Nat Chem Biol. 2019;15(12):1137–47.
6. Tsurusaki S, Tsuchiya Y, Koumura T, Nakasone M, Sakamoto T, Matsuoka M, et al. Hepatic ferroptosis plays an important role as the trigger for initiating inflammation in nonalcoholic steatohepatitis. Cell Death Dis. 2019;10(6):449.

7. Martín-Fernández M, Arroyo V, Carnicero C, Sigüenza R, Busta R, Mora N, et al. Role of Oxidative Stress and Lipid Peroxidation in the Pathophysiology of NAFLD. Antioxidants (Basel). 2022;11(11).
8. Qi J, Kim JW, Zhou Z, Lim CW, Kim B. Ferroptosis Affects the Progression of Nonalcoholic Steatohepatitis via the Modulation of Lipid Peroxidation-Mediated Cell Death in Mice. Am J Pathol. 2020;190(1):68–81.
9. Sun X, Ou Z, Chen R, Niu X, Chen D, Kang R, et al. Activation of the p62-Keap1-NRF2 pathway protects against ferroptosis in hepatocellular carcinoma cells. Hepatology. 2016;63(1):173–84.
10. Pan C, Hou W, Deng X, Liu J, Chi R, Shang X, et al. The Pivotal Role of Nrf2 Signal Axis in Intervertebral Disc Degeneration. J Inflamm Res. 2023;16:5819–33.
11. Tang D, Chen X, Kang R, Kroemer G. Ferroptosis: molecular mechanisms and health implications. Cell Res. 2021;31(2):107–25.
12. Ding Y, Chen X, Liu C, Ge W, Wang Q, Hao X, et al. Identification of a small molecule as inducer of ferroptosis and apoptosis through ubiquitination of GPX4 in triple negative breast cancer cells. J Hematol Oncol. 2021;14(1):19.
13. Yin X, Liu Z, Li C, Wang J. Hinokitiol ameliorates MASH in mice by therapeutic targeting of hepatic Nrf2 and inhibiting hepatocyte ferroptosis. Phytomedicine. 2025;139:156472.
14. Chen Z, Zhang Z, Liu J, Qi H, Li J, Chen J, et al. Gut Microbiota: Therapeutic Targets of Ginseng Against Multiple Disorders and Ginsenoside Transformation. Front Cell Infect Microbiol. 2022;12:853981.
15. Yang C, He X, Zhao J, Huang W. Hepatoprotection by Ginsenoside Rg1 in alcoholic liver disease. Int Immunopharmacol. 2021;92:107327.
16. Mo C, Xie S, Zeng T, Lai Y, Huang S, Zhou C, et al. Ginsenoside-Rg1 acts as an IDO1 inhibitor, protects against liver fibrosis via alleviating IDO1-mediated the inhibition of DCs maturation. Phytomedicine. 2021;84:153524.
17. Zhou H, Liu Y, Su Y, Ji P, Kong L, Sun R, et al. Ginsenoside Rg1 attenuates lipopolysaccharide-induced chronic liver damage by activating Nrf2 signaling and inhibiting inflammasomes in hepatic cells. Journal of Ethnopharmacology. 2024;324.
18. Wei X, Chen Y, Huang W. Ginsenoside Rg1 ameliorates liver fibrosis via suppressing epithelial to mesenchymal transition and reactive oxygen species production in vitro and in vivo. BioFactors. 2018;44(4):327–35.
19. Chen X, Xue W, Zhang J, Peng J, Huang W. Ginsenoside Rg1 attenuates the NASH phenotype by regulating the miR-375-3p/ATG2B/PTEN-AKT axis to mediate autophagy and pyroptosis. Lipids Health Dis. 2023;22(1):22.
20. Zhang R, Li X, Gao Y, Tao Q, Lang Z, Zhan Y, et al. Ginsenoside Rg1 Epigenetically Modulates Smad7 Expression in Liver Fibrosis via MicroRNA-152. J Ginseng Res. 2023;47(4):534–42.
21. Day CP, James OF. Steatohepatitis: a tale of two "hits"? Gastroenterology. 1998;114(4):842–5.

22. Buzzetti E, Pinzani M, Tsochatzis EA. The multiple-hit pathogenesis of non-alcoholic fatty liver disease (NAFLD). Metabolism. 2016;65(8):1038–48.
23. Li X, Wang TX, Huang X, Li Y, Sun T, Zang S, et al. Targeting ferroptosis alleviates methionine-choline deficient (MCD)-diet induced NASH by suppressing liver lipotoxicity. Liver Int. 2020;40(6):1378–94.
24. Chen W, Balan P, Popovich DG. Comparison of Ginsenoside Components of Various Tissues of New Zealand Forest-Grown Asian Ginseng (Panax Ginseng) and American Ginseng (Panax Quinquefolium L.). Biomolecules. 2020;10(3).
25. Qin Q, Lin N, Huang H, Zhang X, Cao X, Wang Y, et al. Ginsenoside Rg1 ameliorates cardiac oxidative stress and inflammation in streptozotocin-induced diabetic rats. Diabetes Metab Syndr Obes. 2019;12:1091–103.
26. Wang Z, Du K, Hou J, Xiao H, Hu L, Chen X, et al. Rg1 alleviates oxidative stress and spermatogonium apoptosis in D-gal-induced testicular toxicity by activating Akt. Redox Rep. 2023;28(1):2206197.
27. Rolo AP, Teodoro JS, Palmeira CM. Role of oxidative stress in the pathogenesis of nonalcoholic steatohepatitis. Free Radic Biol Med. 2012;52(1):59–69.
28. Allameh A, Niayesh-Mehr R, Aliarab A, Sebastiani G, Pantopoulos K. Oxidative Stress in Liver Pathophysiology and Disease. Antioxidants (Basel). 2023;12(9).
29. Zhu Z, Zhang Y, Huang X, Can L, Zhao X, Wang Y, et al. Thymosin beta 4 alleviates non-alcoholic fatty liver by inhibiting ferroptosis via up-regulation of GPX4. Eur J Pharmacol. 2021;908:174351.
30. Gao H, Jin Z, Bandyopadhyay G, Wang G, Zhang D, Rocha KCE, et al. Aberrant iron distribution via hepatocyte-stellate cell axis drives liver lipogenesis and fibrosis. Cell Metab. 2022;34(8):1201–13.e5.
31. Illés E, Patra SG, Marks V, Mizrahi A, Meyerstein D. The Fe(II)(citrate) Fenton reaction under physiological conditions. J Inorg Biochem. 2020;206:111018.
32. Guan Q, Wang Z, Hu K, Cao J, Dong Y, Chen Y. Melatonin Ameliorates Hepatic Ferroptosis in NAFLD by Inhibiting ER Stress via the MT2/cAMP/PKA/IRE1 Signaling Pathway. Int J Biol Sci. 2023;19(12):3937–50.
33. Kong L, Liu Y, Li J, Wang Y, Ji P, Shi Q, et al. Ginsenoside Rg1 alleviates chronic inflammation-induced neuronal ferroptosis and cognitive impairments via regulation of AIM2 - Nrf2 signaling pathway. J Ethnopharmacol. 2024;330:118205.
34. Wang Y, Yan S, Liu X, Deng F, Wang P, Yang L, et al. PRMT4 promotes ferroptosis to aggravate doxorubicin-induced cardiomyopathy via inhibition of the Nrf2/GPX4 pathway. Cell Death Differ. 2022;29(10):1982–95.
35. Zhu W, Tang H, Cao L, Zhang J, Li J, Ma D, et al. Epigallocatechin-3-O-gallate ameliorates oxidative stress-induced chondrocyte dysfunction and exerts chondroprotective effects via the Keap1/Nrf2/ARE signaling pathway. Chem Biol Drug Des. 2022;100(1):108–20.
36. Tsai KJ, Tsai HY, Tsai CC, Chen TY, Hsieh TH, Chen CL, et al. Luteolin Inhibits Breast Cancer Stemness and Enhances Chemosensitivity through the Nrf2-Mediated Pathway. Molecules.

2021;26(21).
37. Zhang Z, Yang K, Mao R, Zhong D, Xu Z, Xu J, et al. Ginsenoside Rg1 inhibits oxidative stress and inflammation in rats with spinal cord injury via Nrf2/HO-1 signaling pathway. Neuroreport. 2022;33(2):81–9.
38. Chen Y, Zhang Q, Sun L, Liu H, Feng J, Li J, et al. Ginsenoside Rg1 attenuates dextran sodium sulfate-induced ulcerative colitis in mice. Physiol Res. 2023;72(6):783–92.
39. Xu S, Chen Y, Miao J, Li Y, Liu J, Zhang J, et al. Esculin inhibits hepatic stellate cell activation and CCl(4)-induced liver fibrosis by activating the Nrf2/GPX4 signaling pathway. Phytomedicine. 2024;128:155465.
40. Shi M, Guo Y, Xu J, Yan L, Li X, Liu R, et al. Gaudichaudione H ameliorates liver fibrosis and inflammation by targeting NRF2 signaling pathway. Free Radic Biol Med. 2024;224:770–84.
41. Yu H, Yan S, Jin M, Wei Y, Zhao L, Cheng J, et al. Aescin can alleviate NAFLD through Keap1-Nrf2 by activating antioxidant and autophagy. Phytomedicine. 2023;113:154746.
42. Ma T, Du J, Zhang Y, Wang Y, Wang B, Zhang T. GPX4-independent ferroptosis-a new strategy in disease's therapy. Cell Death Discov. 2022;8(1):434.
43. Zhang M, Liu J, Yu Y, Liu X, Shang X, Du Z, et al. Recent Advances in the Inhibition of Membrane Lipid Peroxidation by Food-Borne Plant Polyphenols via the Nrf2/GPx4 Pathway. J Agric Food Chem. 2024;72(22):12340–55.

Figures

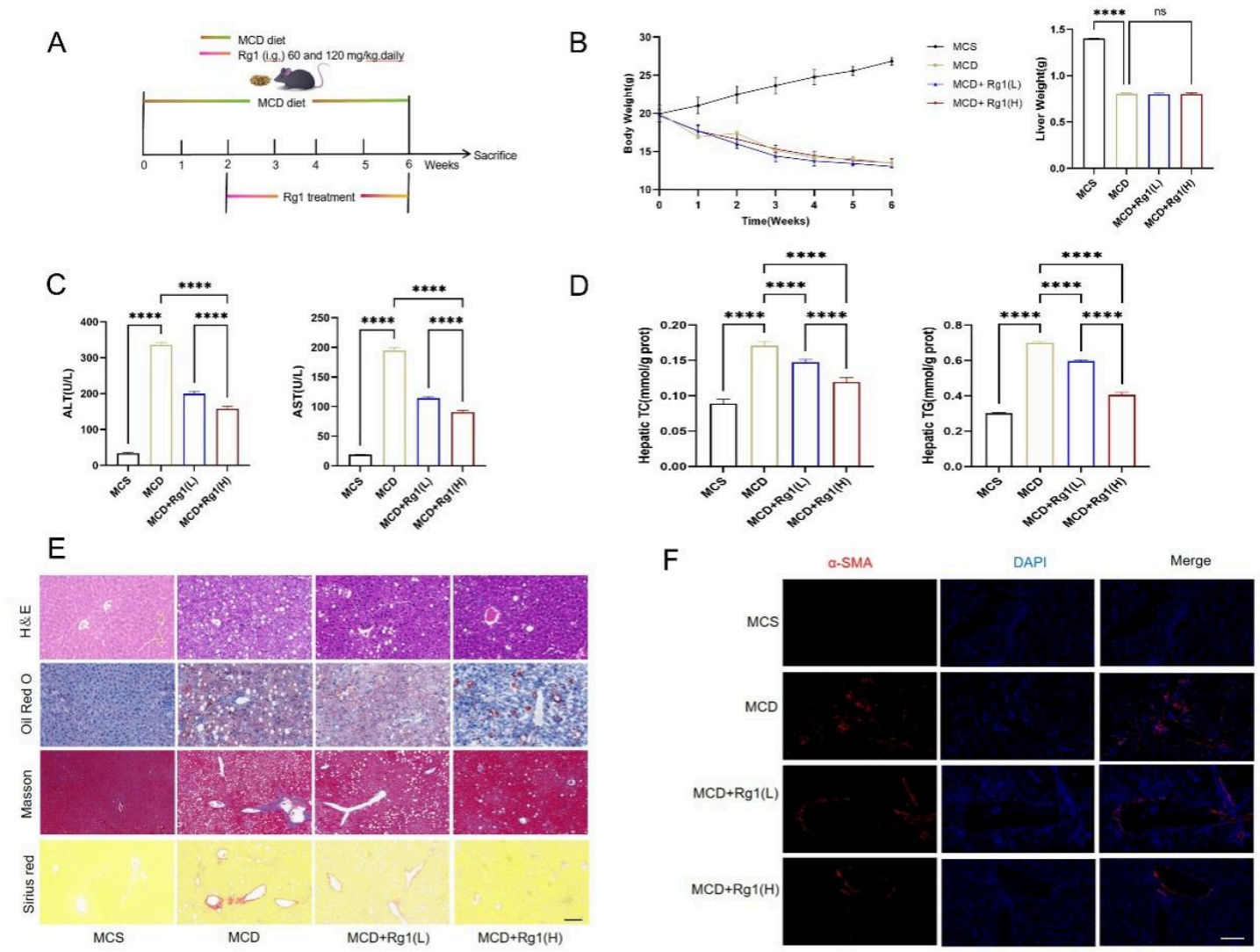


Figure 1

Rg1 alleviates MCD-induced liver injury in mice (A) Diagrammatic representation of the experimental processes. (B)Body weight and liver weight. (C)Serum ALT and serum AST levels. (D)Liver TC and liver TG levels. (E) H&E staining, Oil Red O staining, Masson's staining, and Sirius Red staining. Scale bar, 100μm. (F)Immunofluorescence of α-SMA expression in liver slices. Scale bar, 200μm. ns p□0.05, ****p < 0.0001.

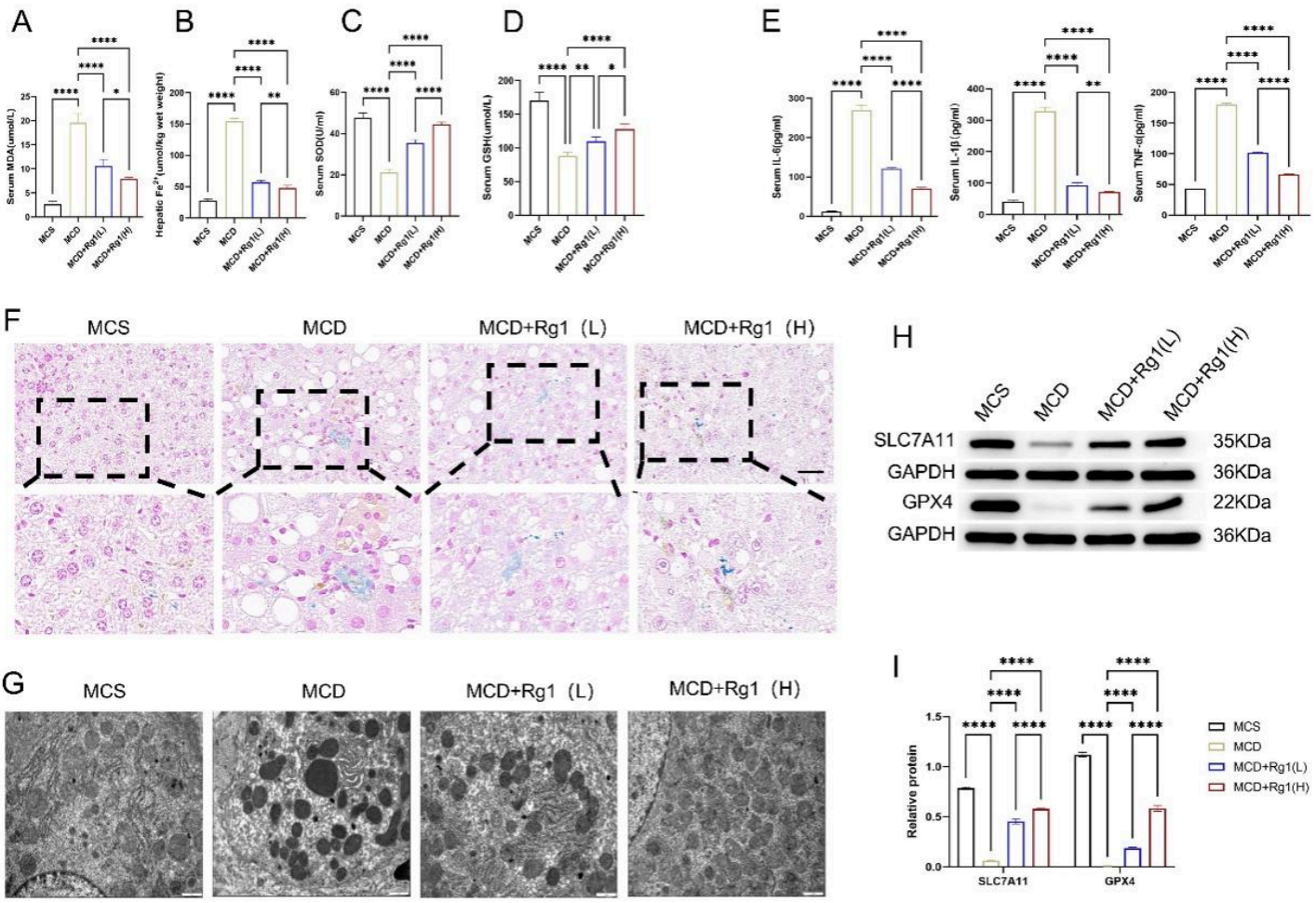


Figure 2

The effect of Rg1 on inflammation and oxidative stress-induced ferroptosis in mice (A)Serum MDA levels. (B)Liver Fe^{2+}levels. (C)Serum SOD levels. (D)Serum GSH levels. (E)Serum levels of IL-6, IL-1β, and TNF-α. (F)Prussian blue staining of liver slices. scale bars, 50μm. (G)Observation of mitochondrial ultrastructure using transmission electron microscopy. scale bar,1μm. (H)Western blot analysis of SLC7A11 and GPX4 protein expression. (I)Quantitative analysis of Western blot bands. *p < 0.05, **p < 0.01, ****p < 0.0001.

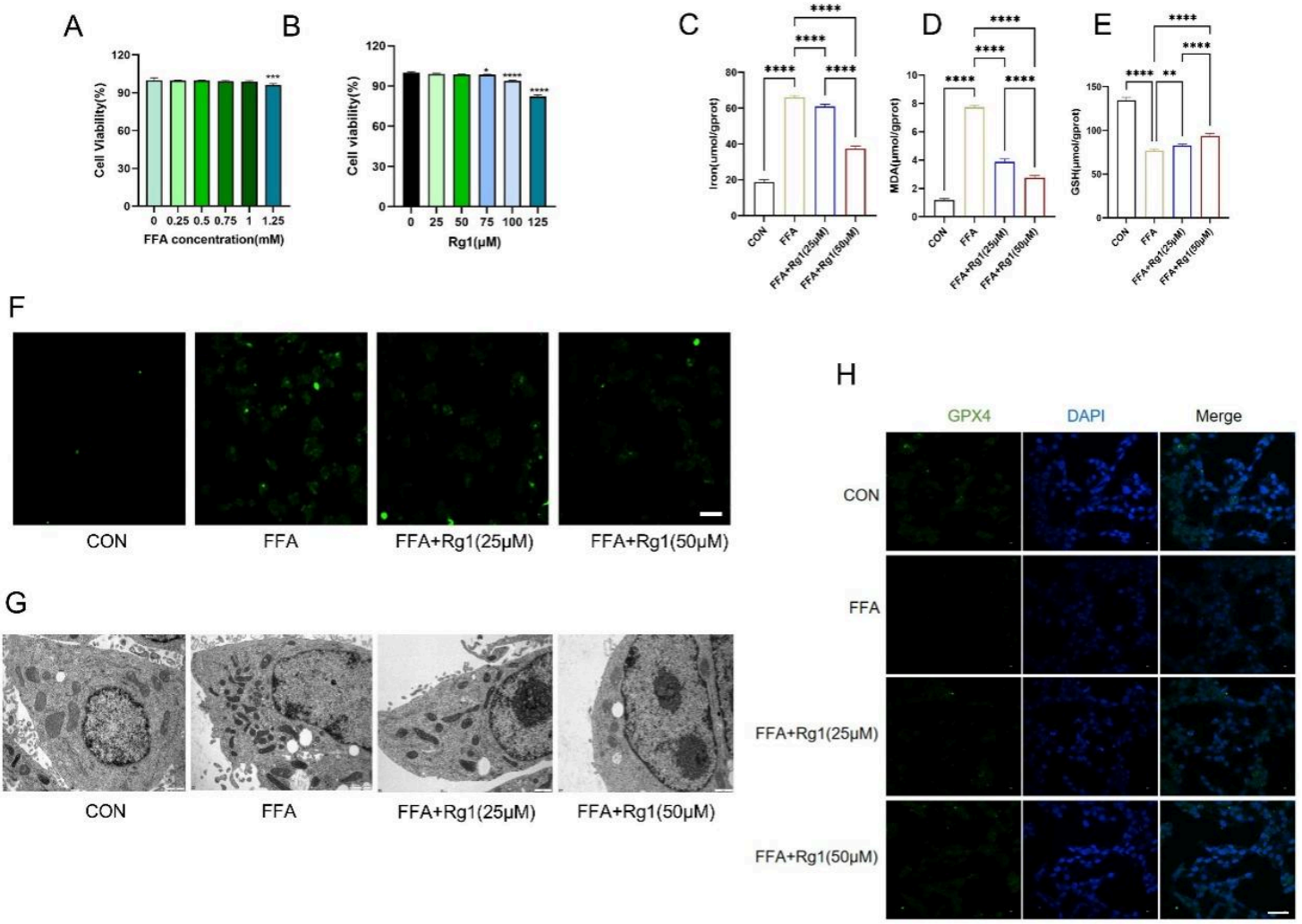


Figure 3

Rg1 inhibits ferroptosis in FFA-induced HepG2 cells. (A-B)After treating HepG2 cells with different concentrations of Rg1 and FFA for 24 hours, cell viability was assessed using the CCK-8 assay. (C)Iron content in cell lysate. (D)MDA levels in cell lysates. (E)GSH levels in cell lysates. (F)Detection of ROS using the DCFH-DA probe. scale bar, 100μm. (G)Observation of mitochondria in the control group and the Rg1-treated group via TEM. scale bar, 1μm. (H)Representative images of GPX4 immunofluorescence staining in HepG2 cells. scale bar, 100μm. *p < 0.05, **p < 0.01, ***p < 0.001, ****p < 0.0001.

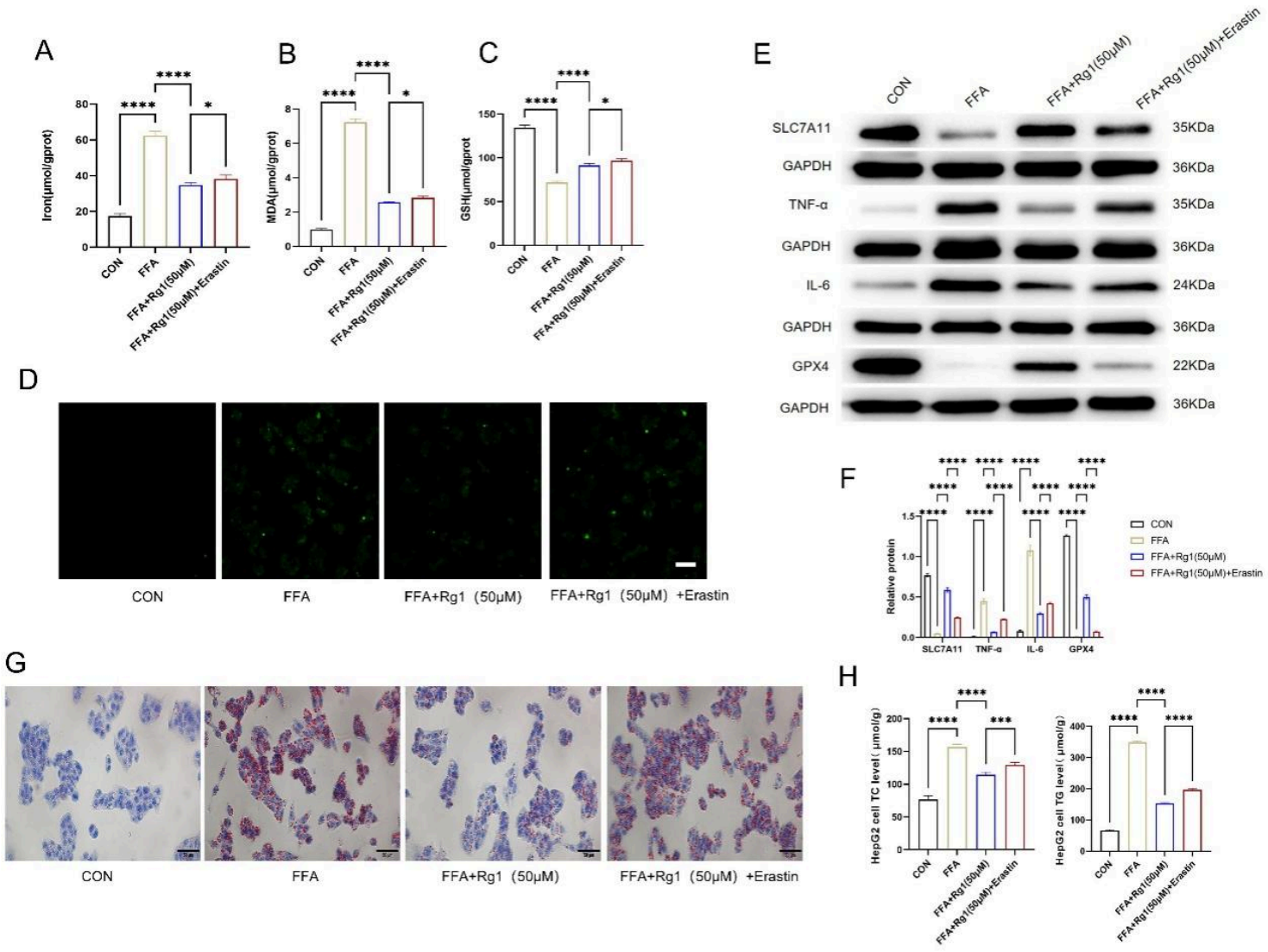


Figure 4

Inducing ferroptosis exacerbates inflammation, oxidative stress, and lipid accumulation in FFA-induced HepG2 cells. HepG2 cells were treated with 1 mM FFA, and then Rg1 (50 μM) or Rg1 (50 μM)+ Erastin (20 μM) were added for 24 h. The levels of iron (A), MDA (B), and GSH (C) in the cell lysates were measured. (D)The DCFH-DA probe was used to detect intracellular ROS levels. scale bar, 100μm. (E-F)Western blot analysis of the expression of SLC7A11, GPX4, TNF - α, and IL-6 proteins. (G)Observation of Lipid Deposition in HepG2 Cells by Oil Red O Staining. scale bar, 50μm. (H)TC and TG levels in cell lysate. *p < 0.05, ***p < 0.001, ****p < 0.0001.

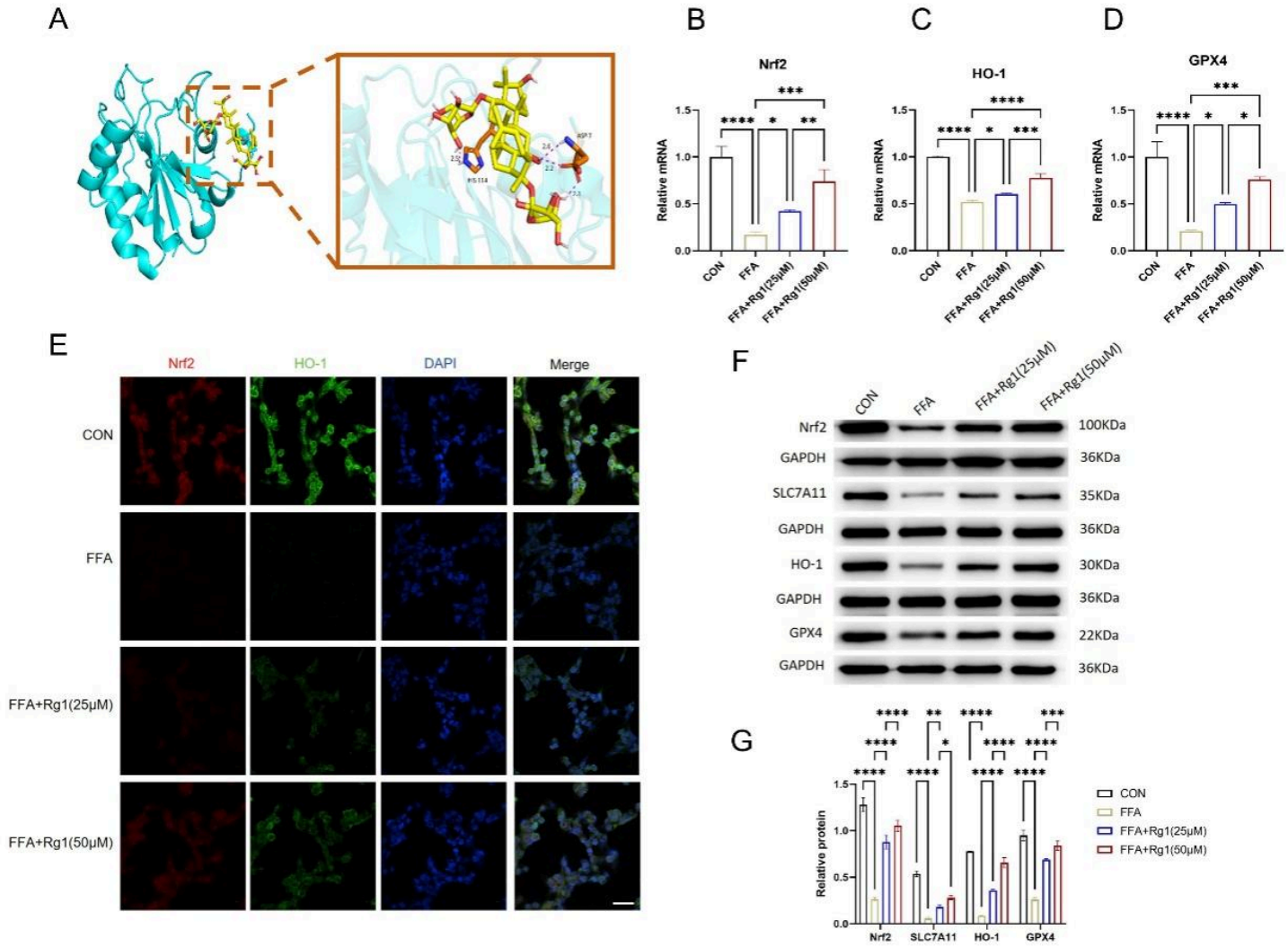


Figure 5

Rg1 inhibits FFA-induced ferroptosis in HepG2 cells by regulating the Nrf2/GPX4 signaling pathway (A)Molecular docking of Rg1 and Nrf2 proteins (B)mRNA expression of Nrf2 in HepG2 cells. (C)mRNA expression of HO-1 in HepG2 cells. (D)mRNA expression of GPX4 in HepG2 cells. (E)Representative images of immunofluorescence staining for Nrf2 and HO-1 in HepG2 cells. scale bar, 100μm. (F)Western blot analysis of the expression of Nrf2, HO-1, SLC7A11, and GPX4 proteins. (G)Quantify the protein expression of Nrf2, HO-1, SLC7A11, and GPX4 using ImageJ software. *p < 0.05, **p < 0.01, ***p < 0.001, ****p < 0.0001.

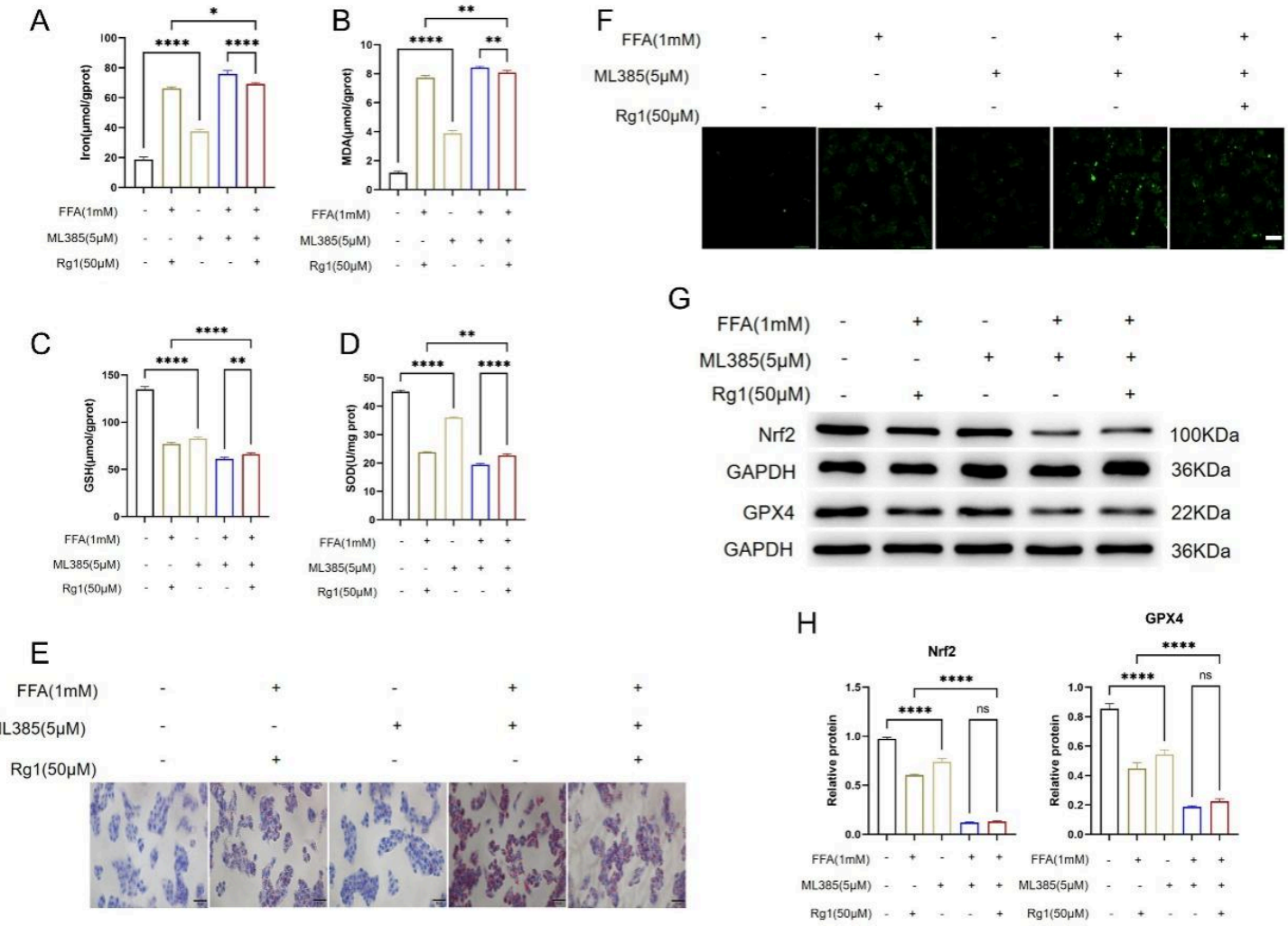


Figure 6

Rg1 inhibits FFA-induced lipid accumulation and oxidative stress in HepG2 cells via Nrf2-mediated ferroptosis. The HepG2 cells were treated with ML385(5μM) or Rg1（50 μM） with or without FFA for 24 h. (A)Iron content in cell lysates. (B)MDA levels in cell lysates. (C)GSH levels in cell lysates. (D) SOD levels in cell lysates. (E)Oil Red O staining of HepG2 cells. scale bar, 50μm. (F)Detection of ROS in HepG2 cells. scale bar, 100μm. (G). Western blot analysis of Nrf2 and GPX4 protein expression in HepG2 cells. (H)Quantification of Nrf2 and GPX4 proteins in HepG2 cells. ns p＞0.05, *p < 0.05, **p < 0.01, ****p < 0.0001.

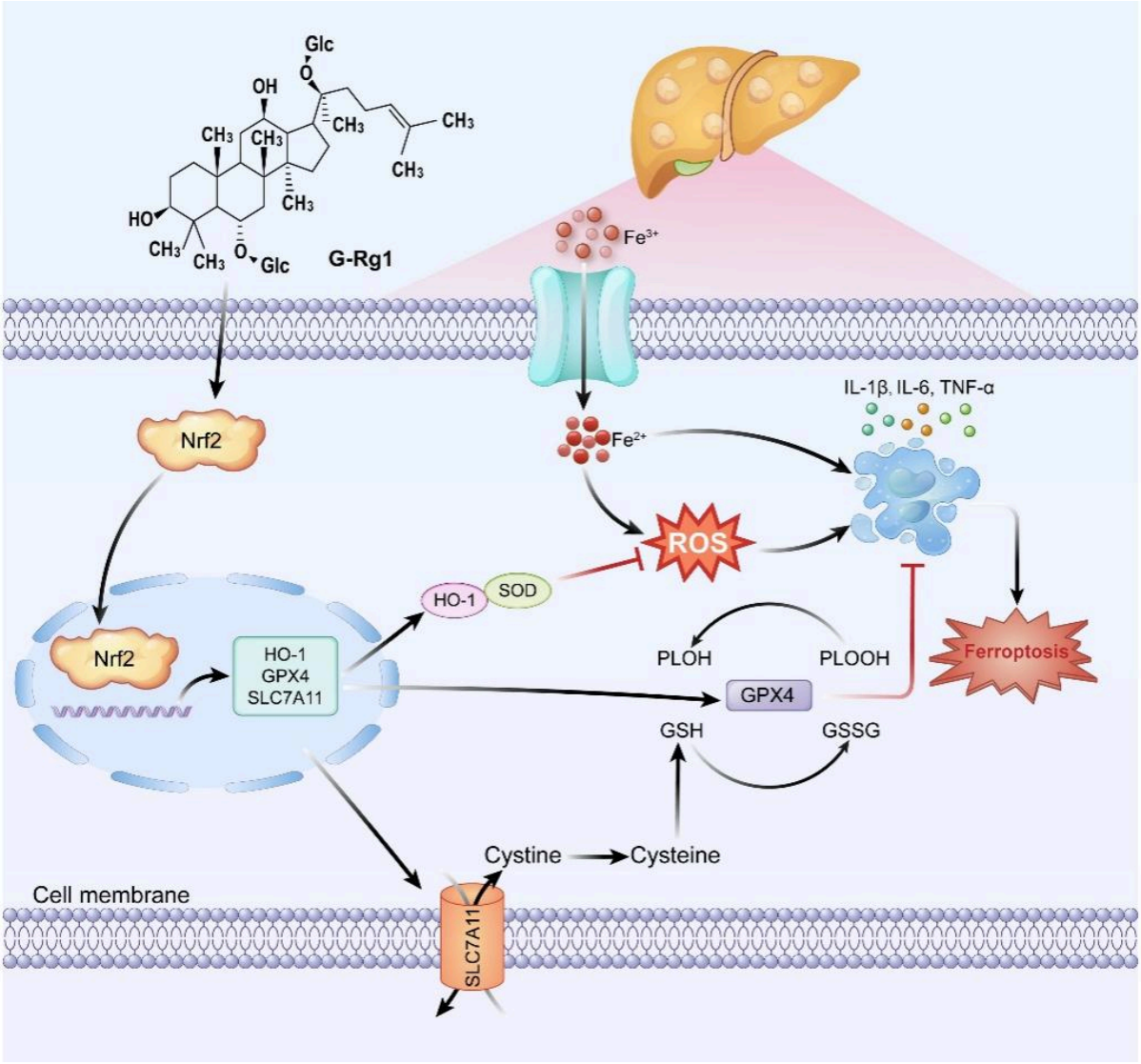


Figure 7

Rg1 alleviates hepatic oxidative stress by enhancing the Nrf2-mediated antioxidant system and upregulating GPX4-mediated anti-ferroptosis, thereby reducing MAFLD-induced liver injury.

Supplementary Files

This is a list of supplementary files associated with this preprint. Click to download.

- SupplementaryMaterial1.pdf